Supporting Information

Synergistic Molecular and Heterojunction Engineering of Sulfonyl-Functionalized Perylene Diimide Polymers for Enhanced Visible-Light Photocatalysis

Yanrong Lu,[a] Zibin Li,[a] Jiajing Feng,*[a] Lihua Guo,[a] Shengchen Lv,[b] Hong Shang,[a] Bing Sun,[a] and Xueke Liu[b]

[a] School of Science, China University of Geosciences (Beijing), Beijing 100083, P.R. China.
[b] Department of Applied Chemistry, China Agricultural University, Beijing, 100193, P. R. China.
E-mail: fengjiajing@cugb.edu.cn

Table of Contents

1. Materials and Characterization Methods

Materials. All chemicals and solvents were purchased from commercial suppliers and used without further purification unless otherwise specified.

Gel Permeation Chromatography (GPC). The relative molecular weight of polymers were determined on a PL-GPC200. The molecular weight is determined according to that time of the polymer flow out with the eluent. Generally, a shorter elution time corresponds to a smaller molecular weight. The mobile phase for the test was trichlorobenzene at 150°C.

Fourier Transform Infrared (FT-IR) Spectroscopy. The FT-IR profiles were recorded over the Nicolet iS10. A small amount of the dried sample was placed directly on the sample stage. The spectrum was recorded with 32 scans and a resolution of 4 cm^{-1}. The resulting data were baseline-corrected.

X-ray Diffraction (XRD). The crystal structure of the photocatalyst was obtained by XRD-6000. The measurements were performed on an Empyrean diffractometer operating at 40 kV and 1.6 kW using Cu Kα radiation. The well-ground powder samples were placed into a sample holder. The data were collected in the 2θ range from 5° to 50°.

X-ray Photoelectron Spectroscopy (XPS). XPS analysis was performed on a ESCALab-250Xi. It is a qualitative and semi-quantitative technique. It was used to analyze the elemental composition and chemical states of elements on the material surface. This information helps deduce hybridization, molecular structure, and chemical bonding. Valence band spectra were also obtained. For sample preparation, about 3 mg of powder was pressed between two pieces of 1 cm × 1 cm aluminum foil. The foil with the sample was attached to the sample holder using double-sided adhesive tape. To calibrate for surface adventitious carbon and instrumental shifts, all spectra were referenced by setting the C 1s peak to 284.7 eV.

Surface Area and Porosity Analysis (BET). BET specific surface areas and pore volumes were determined from N_2 adsorption-desorption isotherms collected with a ASAP3020 system at 77 K, pretreatment of sample was activated under vacuum at 120°C for 10 h..

Scanning Electron Microscopy (SEM). SEM imaging of samples were performed on a SU-8010. A small amount of the sample was placed in a 0.5 mL centrifuge tube with 0.25 mL of ethanol. The tube was sealed with parafilm and ultrasonicated for 20 minutes. A drop of the suspension was dripped onto a silicon wafer. After drying, the wafer was sputter-coated with gold before testing.

Transmission Electron Microscopy (TEM). TEM imaging of samples were performed on a JEM-2100F. A small amount of the sample was dispersed in 0.25 mL of ethanol within a 0.5 mL centrifuge tube. The tube was sealed with parafilm and ultrasonicated for 20 minutes. A drop of the suspension was then deposited onto a microgrid copper mesh and dried.

Ultraviolet-Visible (UV-Vis) Spectroscopy. UV-Vis adiffuse reflectance spectroscopy (DRS) were measured with Lambda 750. It was used to study the band gap and absorption spectra of the prepared photocatalysts. A background measurement was first taken with barium sulfate in an integrating sphere. Approximately 20 mg of the sample was then spread evenly on the barium sulfate surface. The measurement was conducted in the range of 200 to 800 nm with a step size of 1 nm.

Electrochemical Measurements. Electrochemical properties, including transient photocurrent response, electrochemical impedance spectroscopy (EIS), and Mott-Schottky analysis, were measured using a CHI760E electrochemical workstation.

The working electrode was prepared as follows. 3 mg of the PDI photocatalyst was dispersed in a mixture of 1 mL of ethanol and 10 μL of Nafion by ultrasonication for 20 minutes. Then, 20 μL of the well-dispersed suspension was drop-cast onto a 1 × 2 cm indium tin oxide (ITO) glass slide and dried under an infrared lamp.

A standard three-electrode system was used for the electrochemical tests. A platinum wire served as the counter electrode, and an Ag/AgCl electrode was used as the reference electrode. The electrolyte was a 0.5 mol L^{-1} Na_2SO_4 aqueous solution. A 300 W xenon lamp from Beijing Perfectlight Technology Co., Ltd., equipped with an AM 1.5G filter, was used as the light source for the open-circuit potential and photocurrent tests. The light was incident perpendicularly onto the front surface of the ITO electrode. Both the EIS and Mott-Schottky measurements were conducted in the dark.

Theoretical calculations. Theoretical calculations were performed to investigate the model catalysts. The structures of the PPDI dimer and trimer were constructed using GaussView 6.0. Geometry optimization and frequency calculations were then conducted using Gaussian 16 software with density functional theory (DFT) at the B3LYP/6-31G* level. Subsequently, the HOMO-LUMO orbitals and energy levels were visualized and analyzed in GaussView 6.0.

Photocatalytic Degradation Experiment. The photocatalytic degradation activity of the catalysts was evaluated using a multi-channel photocatalytic reactor (CEL-LB70) with Congo red (CR) as the target pollutant. For each test, 10 mg of the catalyst was added to a quartz tube containing 50 mL of a 100 mg L^{-1} CR solution. Before light irradiation, the mixture was stirred in the dark for 30 minutes using the reactor's built-in stirrer to achieve adsorption-desorption equilibrium. Subsequently, photocatalytic degradation was initiated by irradiating the solution with a 500 W xenon lamp equipped with a visible-light filter to simulate visible-light conditions at room temperature. Samples (5 mL each) were extracted from the reaction mixture at specific time intervals. Each sample was first filtered through a 0.22 μm aqueous-phase filter membrane and then analyzed by UV-Vis spectrophotometry to determine the remaining concentration of CR.

The photocatalytic degradation data were processed to plot $\ln(C_0/C)$ versus time (t). According to the pseudo-first-order kinetic model, the slope of this plot corresponds to the apparent rate constant (k).

Mechanistic Investigation Experiments. To elucidate the reaction mechanism during photodegradation, scavenger experiments were conducted to identify the primary active species. Methanol (MeOH), tert-butanol (TBA), and p-benzoquinone (BQ) were introduced into the CR solution as scavengers for holes (h^+), hydroxyl radicals (·OH), and superoxide radicals ($\cdot O_2^-$), respectively.

2. Synthesis Methods

Synthesis of Perylene Diimide Linear Polymers (Taking 3,3'-DS-PPDI as an example): PTCDA (0.78 g, 2 mmol), 3,3′-diaminodiphenyl sulfone (0.496 g, 2 mmol), anhydrous $Zn(OAc)_2$ (0.37 g, 2 mmol) and imidazole (5 g) were charged into a 250 mL Schlenk flask. The mixture was degassed by three evacuation–N_2 refill cycles and left under N_2. The flask was immersed in a liquid-metal bath and heated to 180°C. After imidazole melted and dissolved the solid, the mixture was stirred at 180°C for 12 h. The reaction was cooled to rt, treated with 1 M HCl (250 mL) and stirred overnight. The precipitate was collected by vacuum filtration, washed with water until neutrality, and dried in vacuo at 80°C for 12 h. The crude product was suspended in DMSO (≈ 20 mL), stirred for 10 min, filtered, and washed with DMSO until the filtrate was colourless. The polymer was dried in vacuo at 80°C for 12 h to give 3,3′-DS-PPDI as a dark-red solid (yield 70%). 4,4′-DS-PPDI and 4,4′-B-PPDI were prepared analogously (yield 73 % and 92 %, respectively).

Construction of Heterojunctions: The as-synthesised PPDI polymer (0.20 g) was dispersed in EtOH (9 mL) and H_2O (1 mL) in a 25 mL PTFE liner, sonicated for 20 min, and stirred at 1500 rpm. Tetrabutyl titanate (1 mL) was added dropwise over 5 min and stirring was continued for 6 h. The liner was sealed in a stainless-steel autoclave and heated at 180°C for 3 h. After cooling to rt, the solid was recovered by centrifugation (8000 rpm, 5 min), washed three times with EtOH and H_2O, and dried at 60°C for 12 h. Pure TiO_2 was prepared identically but in the absence of polymer.

3. Experimental Results

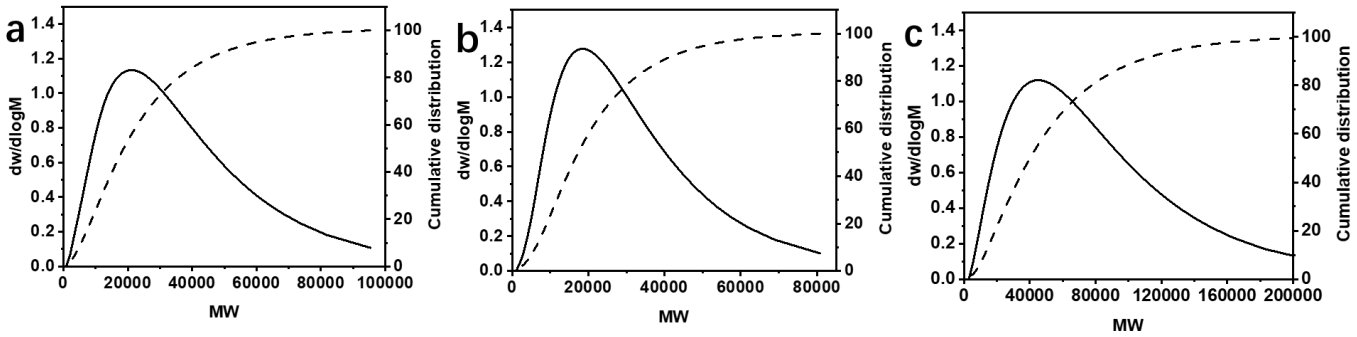

Fig. S1 Molecular weight and molecular distribution of (a) 3,3'-DS-PPDI, (b) 4,4'-DS-PPDI, and (c) 4,4'-B-PPDI in 1,3,5-trichlorobenzene solvent at 150°C by GPC.

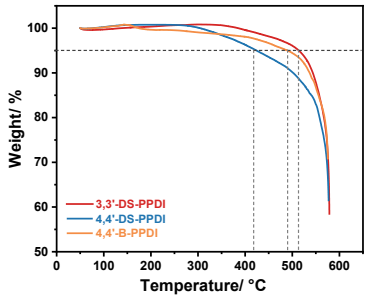

Fig. S2 The TGA plots of 3,3'-DS-PPDI, 4,4'-DS-PPDI and 4,4'-B-PPDI. The decomposition temperature of 5% weight loss are 514°C for 3,3'-DS-PPDI and 418°C for 4,4'-DS-PPDI and 490°C for 4,4'-B-PPDI.

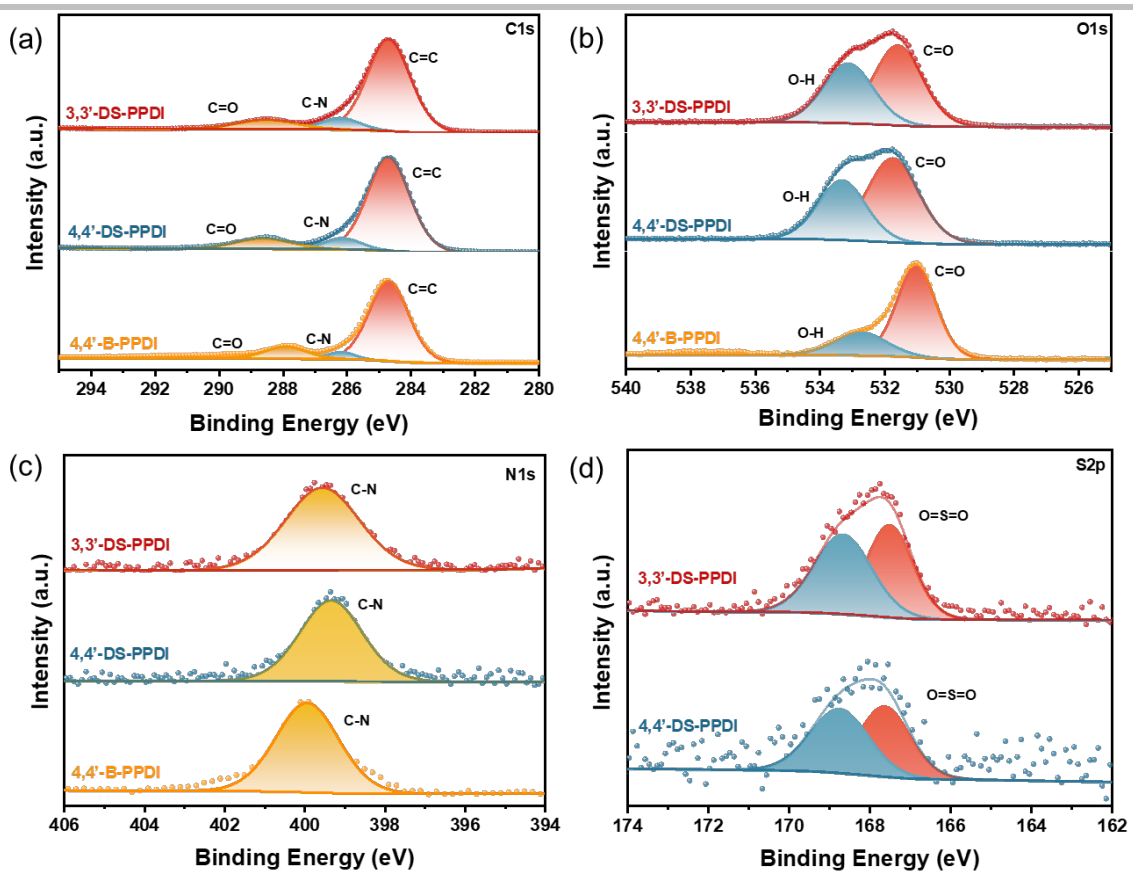

Fig. S3 High-resolution XPS spectra of three PDI polymers.

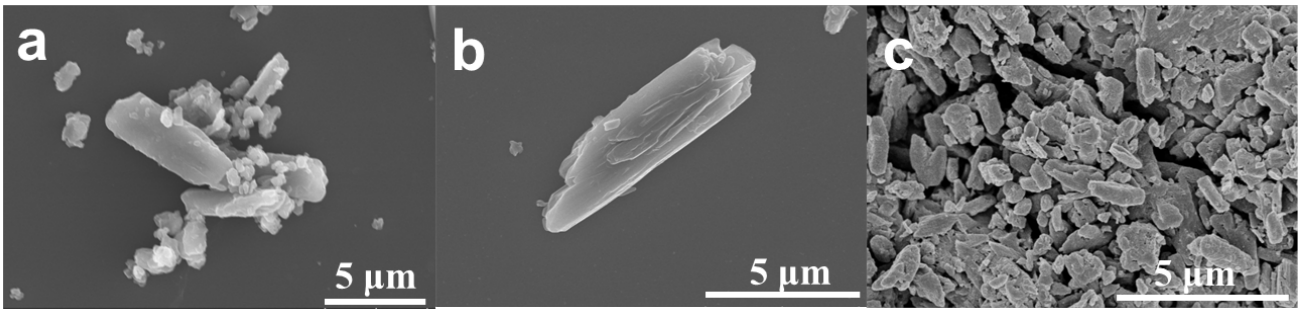

Fig. S4 SEM images of (a) 3,3'-DS-PPDI, (b) 4,4'-DS-PPDI, and (c) 4,4'-B-PPDI.

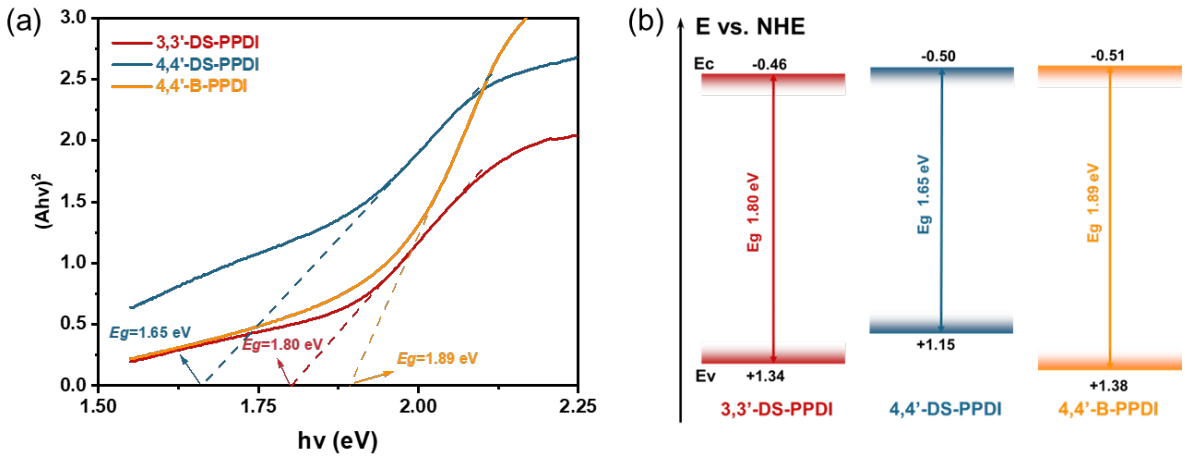

Fig. S5 (a) Tauc plots and (b) energy level diagram of three PDI polymers.

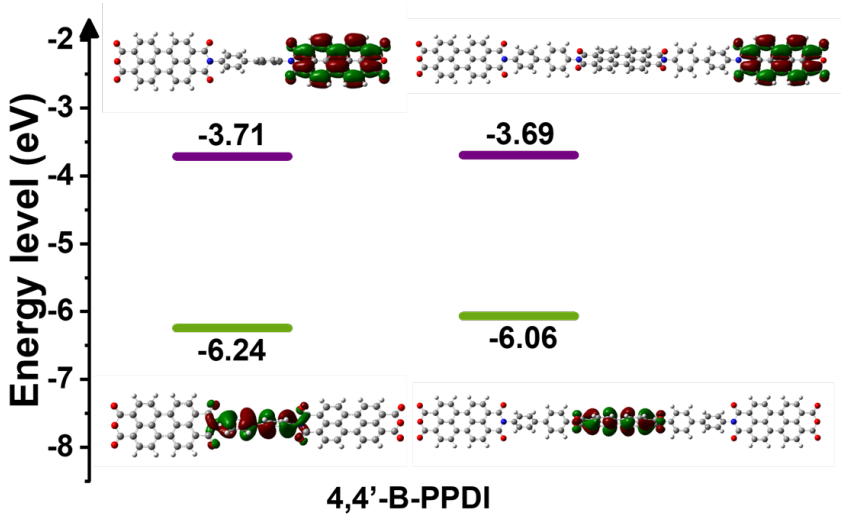

Fig. S6 Optimized molecular structure and the distribution of frontier orbitals of 4,4'-B-PPDI.

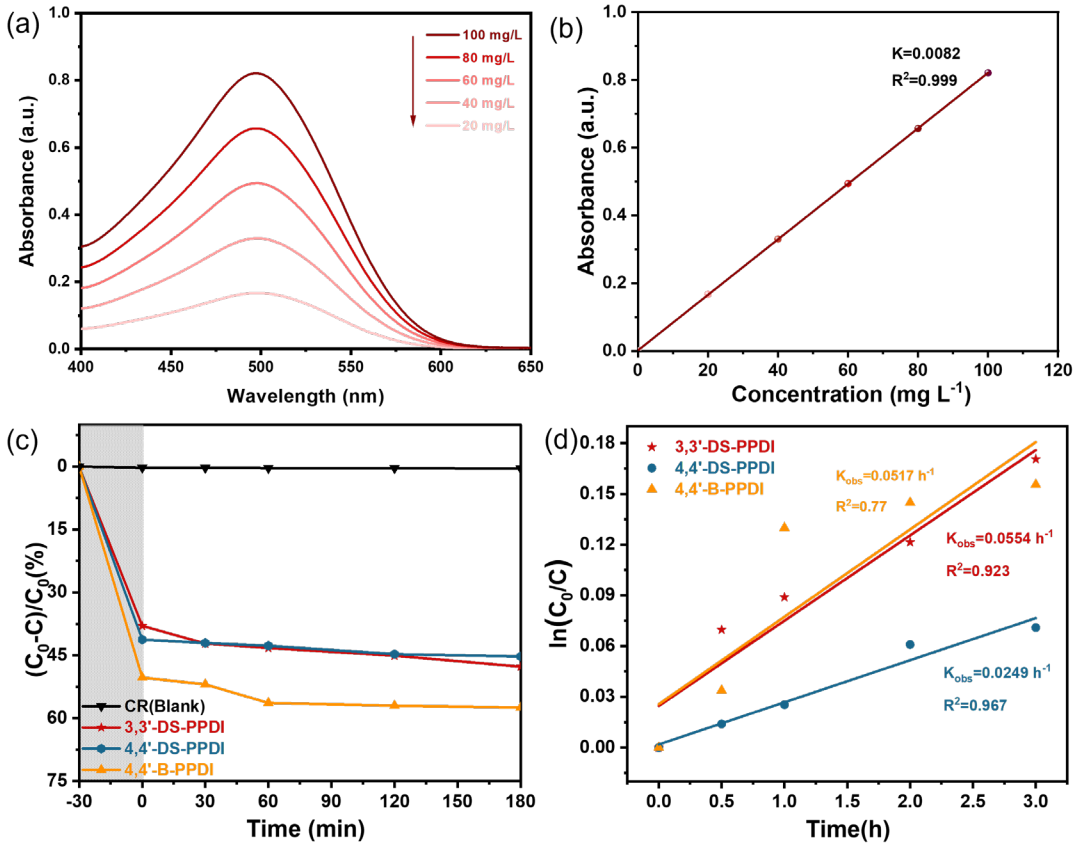

Fig. S7 (a) UV-Vis absorption spectra and (b) absorbance-concentration standard curve of CR at different concentrations. (c) Degradation of CR by different catalysts in visible light, and (d) degradation kinetic curves.

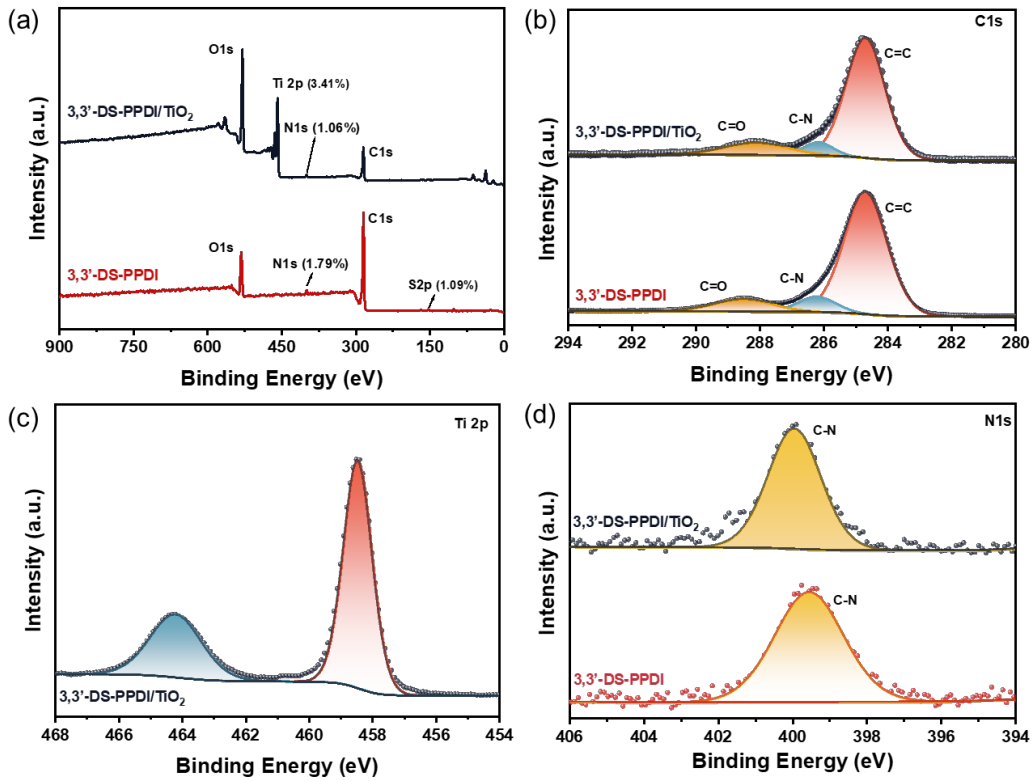

Fig. S8 XPS spectra of 3,3'-DS-PPDI/TiO_2 and 3,3'-DS-PPDI.

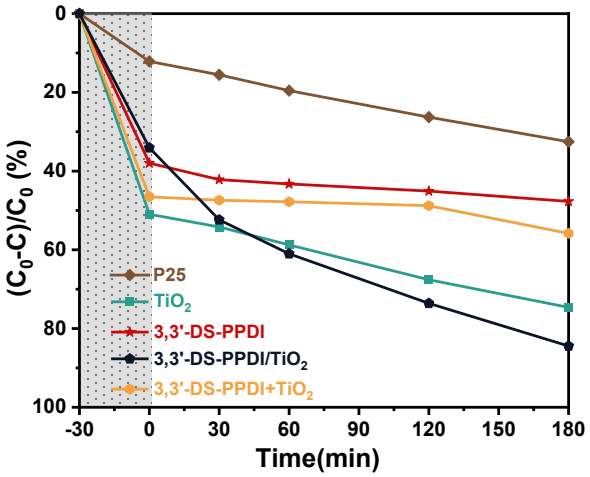

Fig. S9 Degradation of CR by different catalysts in visible light.

Table S1: Comparison of the Photocatalytic Properties of PDI Photocatalysts toward Pollutant Degradation

Photocatalysts	Structure and morphology	The amount of catalysts	Targeted pollutant	Concentration of pollutant	Degradation capability	ref.
3,3'-DS-PPDI/TiO_2	layered architecture	10 mg	CR	100 mg/L	422 mg/g	This work
PDI-COOH	nanobelts	25 mg	MB RhB	40 mg/L 20 mg/L	About 40 mg/g About 20 mg/g	**1**
sAmi-PDI-HCl	2D layers with flaky	25 mg	MB	1×10^{-5} mol/L	About 4.1 mg/g	**2**
PDI_{SA}/AgBr	rod-shaped structure	30 mg	RhB	10 mg/L	16.3 mg/g	**3**
sL-Ala-PDI	nanobelts	25 mg	MB	5×10^{-5} mol/L	About 37.4 mg/g	**4**

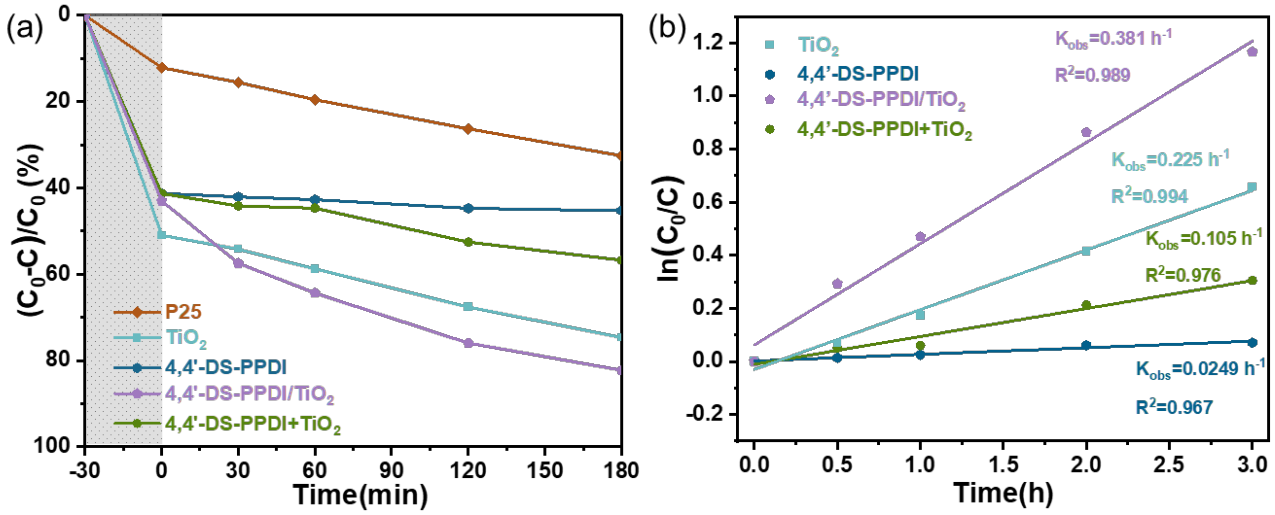

Fig. S10 (a) Degradation of CR by different catalysts in visible light and (b) degradation kinetic curves.

4. References

1. Y. Pu, F. Bao, D. Wang, X. Zhang, Z. Guo, X. Chen, Y. Wei, J. Wang and Q. Zhang, *Journal of Environmental Chemical Engineering*, 2022, **10**, 107123.
2. H. Li, C. Wang, X. Bai, X. Wang, B. Sun, D. Li, L. Zhao, R. Zong and D. Hao, *Mater. Chem. Front.*, 2020, **4**, 2673-2687.
3. T. Xu, S. Zhang, W. Zhang and L. Shi, *Opt. Mater.*, 2024, **147**, 114656.
4. X. Bai, C. Wang, X. Wang, T. Jia, B. Sun, S. Yang, D. Li, J. Li and H. Li, *Catal. Sci. Technol.*, 2021, **11**, 1899-1913.